CITATION:
E. F. Kelley, G. R. Jones, and T. A. Germer, "Display Reflectance Model Based on the BRDF." Displays, Vol. 19, No. 1, June 30, 1998, pp. 27-34 (June 1998).

Display Reflectance Model Based on the BRDF

Edward F. Kelley, George R. Jones, and Thomas A. Germer
NIST, Gaithersburg, MD 20899, USA

ABSTRACT:

Many flat panel displays (FPDs) have anti-reflection surface treatments that differ in character from those of traditional cathode-ray-tube displays. Specular reflection models (mirror-like, producing a distinct image) combined with diffuse (Lambertian) reflection models can be entirely inadequate to characterize the reflection properties of such displays. A third reflection component, called haze, exists between specular and diffuse. Display metrology should account for the haze component of reflection. That is best done using the bidirectional reflectance distribution function (BRDF). The effects of using oversimplified reflectance models are discussed in contrast with a parameterized BRDF.

INTRODUCTION:

Flat panel displays (FPDs) can have reflection properties that differ substantially from their cathode-ray-tube (CRT) counterparts. In the case of the CRT, the necessity of the thick front glass prevents strongly diffusing surface treatments from being used on the front surface. Such treatments, distant from the pixel surface, would compromise readability. With FPDs the front surface can be very close to the pixel surface, permitting surfaces that substantially diffuse incident light without seriously compromising the display's resolution. (This is easy to see: Take wax paper and hold it about 1 cm above some text; compare the readability for that configuration with the readability when the wax paper is placed directly upon the text.) Therefore, CRTs are often made with very mild surface treatments to diffuse the specular light, but their surfaces cannot be as diffusing as those that can be used with some FPDs. Because strongly diffusing surfaces can be used in connection with FPDs, conventional reflection measurement techniques used to characterize display reflection for CRTs may well prove to be inadequate or, at the very least, irreproducible when applied to all FPDs.

In this paper, when we refer to diffuse reflectance, we refer to an ideal Lambertian reflector that obeys the relation:

$$L = qE = E\rho_d/\pi, \tag{1}$$

where L is the luminance, E is the illuminance, $q = \rho_d/\pi$ is the luminance coefficient, and ρ_d is the diffuse (Lambertian) reflectance. That is, the luminance is independent of direction. When we refer to specular reflection, we mean mirror-like reflection that produces a distinct virtual image of the source where the reflected luminance L is related to the source luminance L_s by:

$$L = \rho_s L_s, \tag{2}$$

where ρ_s is the specular reflectance. A more general way to describe reflection is through the bidirectional reflectance distribution function (BRDF). It is the differential form of Eq. 1 and will be developed in the next section. Using the BRDF, we can account for the above specular and diffuse (Lambertian) properties, but also understand a third type of reflection that exists between the two extremes of specular and diffuse (Lambertian) reflection.

This third component of reflection is quickly identified by the eye when it views electronic displays. For want of a better term we will call it haze (see ASTM E284 [1] and D-4449 [2]). Haze reflection is similar to diffuse (Lambertian) reflection in that it depends upon the illuminance (source-display distance), whereas it is similar to specular reflection in that the luminance is peaked in the specular direction. In Fig. 1 we show drawings of the three types of reflection and their combinations. Using a bare bulb of a flashlight placed 200 mm or more in front of the screen, the significant components of the reflection are easily observed and appear distinct from one another. The diffuse (Lambertian) component is seen as an overall gray, as if it were a dark-gray matte paint, slightly brighter where the screen is nearest the source and gradually darker near the edges of the display because of the $1/r^2$ falloff in illuminance. The specular (mirror-like) component is the virtual image of the point source seen in the display surface. The haze component is the distinct fuzzy ball of light that surrounds the specular image. Sometimes the

haze component can be very slight (as with television picture tubes), other times the haze component can be the dominant reflection component (as with many FPDs found in laptop computers).

It is important to realize that not all components of reflection need to be observable. In practice, at least one of the three components must exist (Fig. 1a, b, c). Further, any combination of all three components is possible. There are displays that have almost entirely diffuse (Lambertian) surfaces (e.g., white copy paper—Fig. 1a). There are displays that have no specular component and have only a haze component with the diffuse (Lambertian) component being negligible (10^{-4} or less than the size of the haze reflection peak in the specular direction—Fig. 1c). When the reflection of a point light source is observed in screens having only a haze component, only a fuzzy patch of light is seen in the specular direction, and no distinct image of the source is observed. There are displays that do not have a substantial haze component and exhibit only specular and diffuse (Lambertian) reflections (Fig. 1d). Many television CRT picture tubes are of this nature. In all these cases, a thin-film antireflection coating can be added to further reduce the reflections from the front surface of the screen, making the surface of the display appear quite dark. This is especially true in the case of 1b, 1c, or 1f where the diffuse (Lambertian) component is either absent or negligible. One way to view the BRDF is to direct a narrow laser beam at the screen and view the reflected light against a large white card in a dark room. The distribution of the light on the white card is the projection of the BRDF upon a plane.

The specular and diffuse (Lambertian) components obey the above Eqs. 1 and 2. A more elaborate formalism is required to describe the haze component. When haze is present, the reflection measurement becomes dependent upon virtually every configuration parameter of the apparatus and measurement instrumentation (the distance, orientation, size, and uniformity of the light source; the distance, entrance pupil, field of view, and focus of the light measuring device; etc.[3])

BIDIRECTIONAL REFLECTANCE DISTRIBUTION FUNCTION FORMALISM:

The reflection model offered here is based on the mathematical formalism for the bidirectional reflectance distribution function (BRDF).[4] Only comparatively recently has an effort been made to examine the BRDFs associated with electronic display surfaces in order to better characterize display reflection.[5,6] Neglecting any wavelength and polarization dependence, the BRDF is a function of two directions, the direction of the incident light (θ_i, ϕ_i in spherical coordinates) and the direction from which the reflection is observed (θ_r, ϕ_r in spherical coordinates). Since not all screens exhibit a wavelength independent reflection and because many liquid crystal displays (LCDs) and glare-reducing cover screens for CRTs exhibit polarizing properties, care must be exercised in applying these assumptions. The BRDF relates how any differential element of incident illuminance, dE_i from direction (θ_i, ϕ_i), contributes to a reflected luminance dL_r observed from direction (θ_r, ϕ_r):

$$dL_r(\theta_r,\phi_r) = B(\theta_i,\phi_i,\theta_r,\phi_r)dE_i(\theta_i,\phi_i)\,, \tag{3}$$

where $B(\theta_i, \phi_i, \theta_r, \phi_r)$ is the BRDF. (In the literature the BRDF is often denoted by f_r. We use B to avoid complicated subscripts and confusion with other uses of "f" within the display industry.) By integrating Eq. 3 over all incident directions in space, the luminance $L_r(\theta_r, \phi_r)$ observed from any direction (θ_r, ϕ_r) can be calculated. The illuminance contributions dE_i can be related to luminance sources in the room. For each element of solid angle $dA_i/r_i^2 = d\Omega = \sin\theta_i\, d\theta_i\, d\phi_i$ there is a source luminance $L_i(\theta_i, \phi_i)$ at a distance r_i from the screen producing illuminance

$$dE_i = L_i(\theta_i,\phi_i)\cos\theta_i d\Omega = L_i(\theta_i,\phi_i)\cos\theta_i \sin\theta_i d\theta\, d\phi\,, \tag{4}$$

where the cosine term accounts for the spreading of the illuminance over a larger area as the inclination angle θ from the normal increases.

Methods for obtaining the BRDF are well documented.[7,8] Most often, a collimated beam of light of radiant flux Φ_i is allowed to be incident upon the sample from direction (θ_i, ϕ_i). The radiant flux Φ_r scattered into a direction (θ_r, ϕ_r) and into a solid angle ω (the detector) is measured. The BRDF is then approximately $B = \Phi_r/(\Phi_i \omega \cos\theta_r)$. Generally, both the source and detector cannot be along the normal at the same time since one obscures the other. In practice, the detector is placed a few degrees θ_s off normal, and the peak reflection is observed when the source is θ_s on the other side of normal.

We can capture these three types of reflection explicitly with the BRDF formalism in terms of three additive components

$$B = D + S + H\,, \tag{5}$$

where the components are defined[6] as:

$$D = q = \rho_d / \pi,$$
$$S = 2\rho_s \delta(\sin^2\theta_r - \sin^2\theta_i)\delta(\phi_r - \phi_i \pm \pi), \quad (6)$$
$$H = H(\theta_i, \phi_i, \theta_r, \phi_r).$$

In the specular term the delta functions provide for a mirror-like distinct virtual image of the source in the viewed reflection.[4] When we integrate this three-component BRDF over all incident illumination directions by combining Eqs. 3-6, the reflected luminance is given by

$$L_r(\theta_r, \phi_r) = qE + \rho_s L_s(\theta_r, \phi_r \pm \pi) + \int_0^{2\pi} \int_0^{\pi/2} H(\theta_i, \phi_i, \theta_r, \phi_r) L_i(\theta_i, \phi_i) \cos(\theta_i) d\Omega. \quad (7)$$

The first term on the right hand side of Eq. 7 is the familiar Lambertian reflection where E is the total illuminance from all directions. The second term is the familiar specular reflection where the specification of $(\theta_r, \phi_r \pm \pi)$ simply selects the light from the viewing direction (θ_r, ϕ_r) reflected about the normal (z-axis), i.e., the specular direction associated with the viewing direction. The last term is the haze contribution. See Fig. 2 for an example of a BRDF taken for the case of Fig. 1g.[9] The ultimate goal of this research is to provide simple methods to obtain a parameterization for the BRDF. Two of those parameters are already familiar—the diffuse (Lambertian) reflectance ρ_d and the specular reflectance ρ_s. We would expect the haze component to be specified by a peak h, a width w at some level, and perhaps several shape parameters a, b, …, etc. The realization of this goal will provide a means to calculate the reflected luminance observed for a display placed in any ambient-light environment.

Display reflections allow us to take advantage of some simplifications: Most displays are viewed from the normal or nearly normal direction, and the range of angles to observe the entire screen from the normal position is usually less than ±30°. It will often be found that the shape of the BRDF does not change dramatically over this viewing-angle range. Thus, a reduced BRDF $B(\theta_i, \phi_i) \equiv B(\theta_i, \phi_i, 0, 0)$ is adequate for most reflection characterizations, and we can drop the subscript "i" in the following, so we can write: $B(\theta, \phi) \equiv B(\theta_i, \phi_i, 0, 0)$. If the BRDF is seen to be axially symmetrical about the specular direction then the BRDF is independent of ϕ, and $B(\theta, \phi) = B(\theta)$. An example of such an in-plane BRDF is shown in Fig. 2. In Fig. 3 we show a comparison of different observation directions for in-plane BRDFs obtained using a display for which there is only a non-trivial haze component of reflection. An illustration of the invariability of the BRDF over the entire viewing surface of the display is found in Fig. 4.

The axial symmetry of the BRDF is one simplification that we are not always able to make for all displays. Because of the pixel matrix structure beneath the front surface, spikes may be observed extending out of the central BRDF profile (see Fig. 5). Such measurements are highly non-trivial. Figure 5 suggests a method to obtain the BRDF by taking a picture of the reflectance of a point light source using a calibrated electronic camera, and determining the needed profiles from an analysis of the picture. However, with this procedure, the measurement might be corrupted by veiling glare from the camera-lens-detector system.

In Fig. 6 we show a comparison between several different types of CRT and FPD displays. (AR refers to a multi-layer anti-reflection coating.) You will note that the CRTs have a specular component that is roughly a factor of ten greater than the maximum haze peak observed for the FPDs. The width of the specular component is indicative of the resolution of the apparatus used (<0.5°). Observe that there are two BRDFs shown for FPD2 for the horizontal and the vertical plane. The pattern observed is very much like that shown in Fig. 5. The vertical BRDF for FPD2 indicates that this display is almost a factor of ten lower in reflectance than the other displays for sources at large angles from the direction of the observer. Indeed, the blackness of this display is impressive even in a bright room. Note also that for the FPDs, the haze peaks appear relatively flat over a ±0.5° or larger region about the specular direction, or so it would seem. This is on a log scale. However, on a linear scale a substantial change is observed over ±0.5° from the specular direction (see Fig. 7).

CONVENTIONAL REFLECTION MEASUREMENTS:

There are three types of reflection measurements commonly employed for electronic displays: large-source diffuse measurements, large-source specular measurements, and small-source specular measurements—see Fig. 8. Let's calculate the luminance measured for each apparatus using the form in Eq. 7. In doing this we will often take advantage of the fact that for small angles, the sine and tangent are approximately equal to the angle in radians.

LARGE-SOURCE DIFFUSE MEASUREMENT: Here we have two uniform lamps each having an exit port of diameter a (radius $r = a/2$ having a subtense of θ_a from the screen, typically 15°) placed at $\pm\theta_s$ (typically 30° or more) on each side of the normal. The detector views the center of the screen from the normal direction. From

Eq. 7 the luminance arises from two factors, the illuminance $E = 2L_s\omega = 2L_s\pi r^2/d^2$ from the lamps, and an integration of the haze over the surface of the lamps:

$$L = 2L_s\left[\rho_d \frac{r^2}{d^2} + \iint_{\text{ExitPort}} H(\theta)\cos\theta\sin\theta\, d\theta\right]. \quad (8)$$

The first term is the luminance from the diffuse (Lambertian) component. The second term is the contribution from the haze. Note, in Fig. 9 how much the haze can vary over the surface of the lamp ($\pm\theta_a/2$) for our two FPDs. To obtain an order of magnitude estimate of the haze term we can use $H(\theta_s)\cos(\theta_s)\pi r^2/d^2$. The approximate expression for the luminance then becomes $L \approx 2L_s r^2[\rho_d + \pi H(\theta_s)\cos(\theta_s)]$. This expression is identical to the expression for the luminance if we permit the diameter of the exit ports of lamps to decrease to 1° so that they can be considered as single sources with solid angle $\omega = \pi r^2/d^2$ each; then we obtain:

$$L = 2L_s \frac{r^2}{d^2}\left[\rho_d + \pi H(\theta_s)\cos\theta_s\right], \quad \text{(small sources)} \quad (9)$$

which is very sensitive to the angle associated with the haze contribution. In Fig. 9 we see that at 30° the haze contributes on the order of 0.007 to the diffuse (Lambertian) term that may be from 0.01 to 0.025 for CRTs and much less (0.001) for many FPDs. The rapid change in the haze reflectance with angle shows why this measurement is sensitive to the angular alignment of the lamps.

LARGE-SOURCE SPECULAR MEASUREMENT: In this case we look in the specular direction at one of the large-diameter sources used in the large-source diffuse measurement (again, typically θ_a = 15° and θ_s is often set at 15°). Equation 7 becomes:

$$L = L_s\left[\rho_d \frac{r^2}{d^2} + \rho_s + 2\pi\int_0^{\theta_a/2=r/d} H(\theta)\cos\theta\sin\theta\, d\theta\right]. \quad (10)$$

Here, the main contribution for displays is from the specular component and the haze component (where we are integrating around the peak of the haze). If we were to examine only the haze profiles, such as in Fig. 7, we might think that since the haze functions are very small at 7.5° and beyond (the typical half angle of the lamp subtense from the screen), that this integral would be relatively insensitive to the size and position of the light source. However, when we look at the integrand, we see the effect of the increase in solid angle with increasing θ for any increment $d\theta$—see Fig. 10. Significant errors can be introduced by a change in position, distance, and uniformity of the lamp used because of the haze contribution. For example, if the subtense of the lamp were to change from 14° to 16° (half angle 7° to 8° in Fig. 10), the haze contribution in Eq. 10 would change by 6 %.

SMALL-SOURCE SPECULAR MEASUREMENT: This is the same configuration as the large-source specular measurement with the diameter of the source subtending approximately 1° or less as viewed from the screen. The source has a solid angle $\omega = \pi r^2/d^2$, and the luminance is:

$$L = qE + \rho_s L_s + hE = (q+h)E + \rho_s L_s = L_s\left[(q+h)\omega + \rho_s\right] = L_s\left[(\rho_d + \pi h)\frac{r^2}{d^2} + \rho_s\right], \quad (11)$$

where h is the peak of the haze profile. Note that as h is on the order of 10 sr^{-1} and the diffuse (Lambertian) reflectance is rarely higher than 0.05, the diffuse term is negligible in both the large-source and small-source specular measurements. Note also how the contribution of the haze depends upon the illuminance as does the diffuse (Lambertian) term. The difference between the large-source and small-source measurements is primarily the extent of the contribution of haze. It is because the diffuse (Lambertian) component is generally not an important factor in Eqs. 10 and 11 that these three measurements can give similar results for displays that look very different to the eye.

Consider Eqs. 10 and 11. Their difference lies in how much of the width of the haze peak is used. If the haze were not present, they would give the same result. We have essentially three variables (at least) and two specular measurements. The three variables (the minimum number) are the haze peak h, the haze width w, and the specular reflectance ρ_s. The large-source specular measurement is sensitive to all three variables, whereas the small-source specular measurement is sensitive only to the specular and the haze peak. We can, therefore, get the same measurements for different looking displays depending upon how these components mix. Adding the large-source diffuse measurement does not alleviate the problem since it adds another variable, the diffuse (Lambertian) reflectance, ρ_d. We then have a total of four variables (at a minimum) and three measurements. This results in the undesirable situation that reflection properties are not sufficiently defined by these measurements to distinguish

displays that can appear very different to the eye. Figure 11 shows two hypothetical displays that would appear very different to the eye in how they reflect light. However, the measured reflected luminance would be the same using the above three techniques. The specular term shown here is related to the specular reflectance by $s = \rho_s/\Omega$, where Ω is the solid angle of the entrance pupil of the detector as viewed from the screen.

POSSIBLE ALTERNATIVES:

Alternative procedures are currently under investigation. These alternative methods are suggested prematurely in order to promote their investigation rather than to definitively prescribe a fully tested metrology for display reflection. Their weaknesses need to be characterized, and their sources of error need to be understood.

These procedures are intended to extract the parameters associated with the BRDF model. The diffuse (Lambertian) parameter would be considered to be the asymptotic lower level the BRDF reaches as the light source is rotated away from the normal as in Fig. 13. This would most likely result from a nonlinear curve fit to the BRDF profile in the cases where a clearly defined plateau is not identifiable at large angles.

The haze peak and specular reflectance might be obtained by observing the reflectance of a distant illuminated annulus subtending 1° or less from the display—see Fig. 13. The specular reflectance might be obtained by subtracting the value of the center of the annulus from the average of the value of the lighted portion and compare the result to the luminance of the source annulus. Unfortunately, glare in the lens system will need to be corrected for an accurate haze-peak measurement. It may be possible to do this by directly viewing the annulus where it subtends the same angular size as that observed in the reflection. With FPDs that can be achieved simply by using a mirror or black glass (appropriately calibrated) at the surface of the display.

The shape of the haze profile may be obtained either from a two-dimensional picture (with corrections for glare), or single measurements of the reflectance at wide angles. For example, once the haze peak is obtained from the annulus apparatus, it may be only necessary to obtain the angle at which the reflectance is 1/10 the value of the haze peak, or at a few other points, in order to characterize the shape of the haze profile adequately. Exactly what will be required remains to be determined. Currently the functions that we have been using to fit the haze profiles are of two forms:

$$H(\theta) = \frac{h}{1+\left|\theta/w\right|^n + b\left|\theta/u\right|^m}, \quad \text{or} \quad H(\theta) = h\left[\frac{1-b}{1+\left|\theta/w\right|^n} + \frac{b}{1+\left|\theta/u\right|^n}\right]. \tag{12}$$

The widths w and u are often very narrow in this formulation. The profiles shown in Fig. 7 have been fit with the first function (see Table 1). (Note that these fitting parameters are for illustration purposes only and do not constitute an accurate measurement of reflection.) It is hoped that more useful functions can be developed that will provide precise assignment of the parameters. As it is with these functions, there is great latitude in determining the best values for the parameters associated with the b-factor.

Table 1. Reflectance Parameters for FPDs

Parameter	FPD1	FPD2H
h (measured)	14.2	15.9
w	2.45°	0.731°
n	1.17	1.56
b	0.121	5.77
u	1.20°	2.47°
m	2.90	2.42
q (measured)	0.00062	0.00065

CONCLUSION:

When we consider the standard measurement techniques in light of the mathematical formulation of the BRDF, we find that those measurements fail to identify the parameters necessary to describe the BRDF. Rather, they tend to be measurements that mix the three components together in ways that do not readily permit the extraction of the functional form of the reflection. We desire to develop simple measurement techniques that will obtain the parameters associated with a mathematical specification of the BRDF. The realization of this goal will provide a means to calculate the reflected luminance observed for a display placed in any ambient-light environment. Also, when we consider an ergonomic study of the reflection of display surfaces, we want to have a metrology at our disposal that relates to what we see and provides discriminating detail at a reasonably fundamental level. Only when we can specify the mathematically relevant reflection parameters—the diffuse (Lambertian) reflectance ρ_d, the specular (mirror-like) reflectance ρ_s, the haze peak h, haze width w, and any haze shape parameters (a, b, …) can we say that we have unambiguously described reflection in a meaningful and predicable manner. Then the ergonomist can make distinguishing evaluations that are reproducible and relevant to what the eye sees, and then we will have a fully meaningful metrology with which to evaluate display reflection quality.

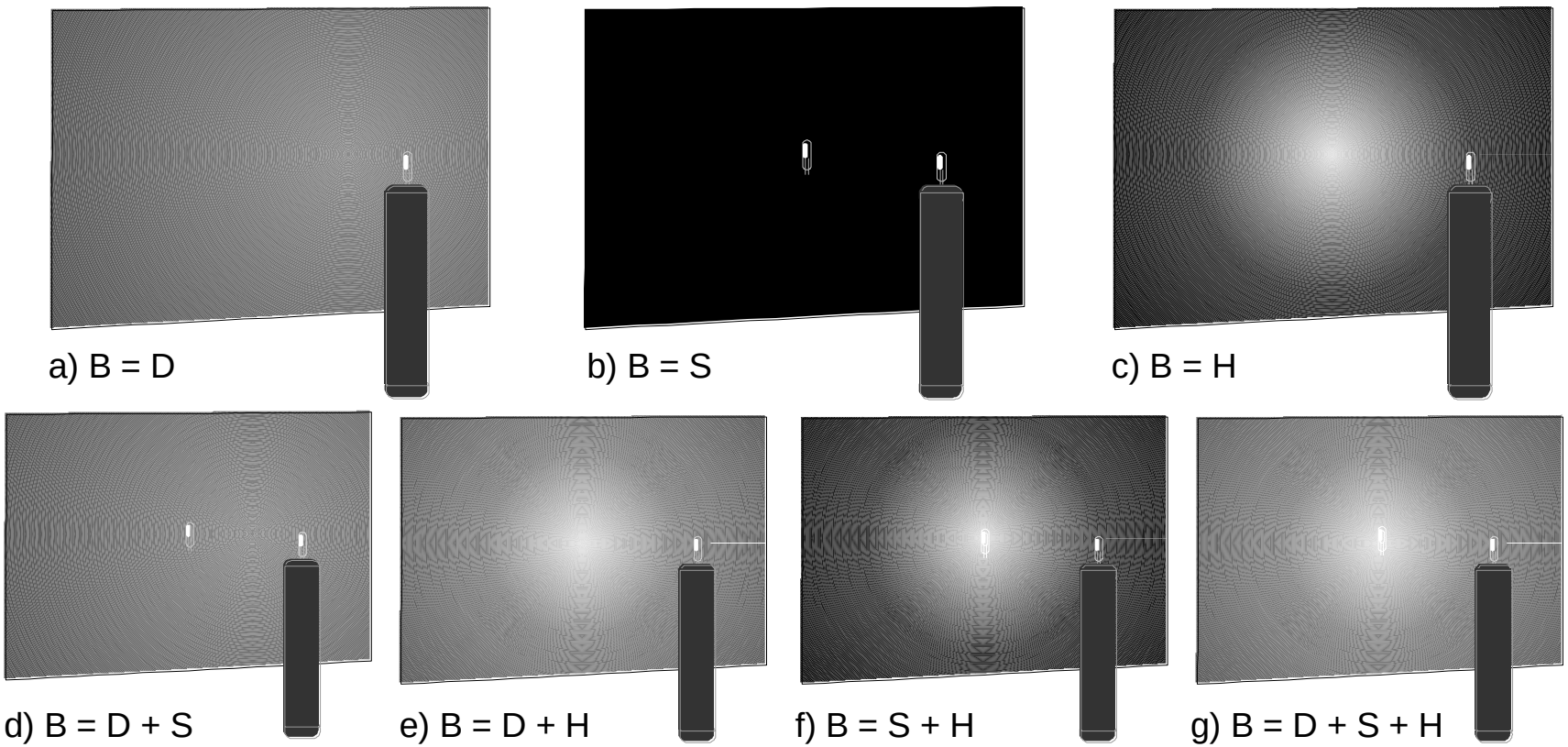

Fig. 1. *Illustration of the three types of reflection found in modern electronic displays. B refers to the BRDF that can have a diffuse (Lambertian) component, D, a mirror-like specular component that produces a distinct image, S, and a haze component, H. At least one component must exist. There are four combinations of the three components. Any or all of the three components can exist nontrivially, or one component can dominate while the other two components make a trivial contribution to the reflection (as in the case of the first three illustrations).*

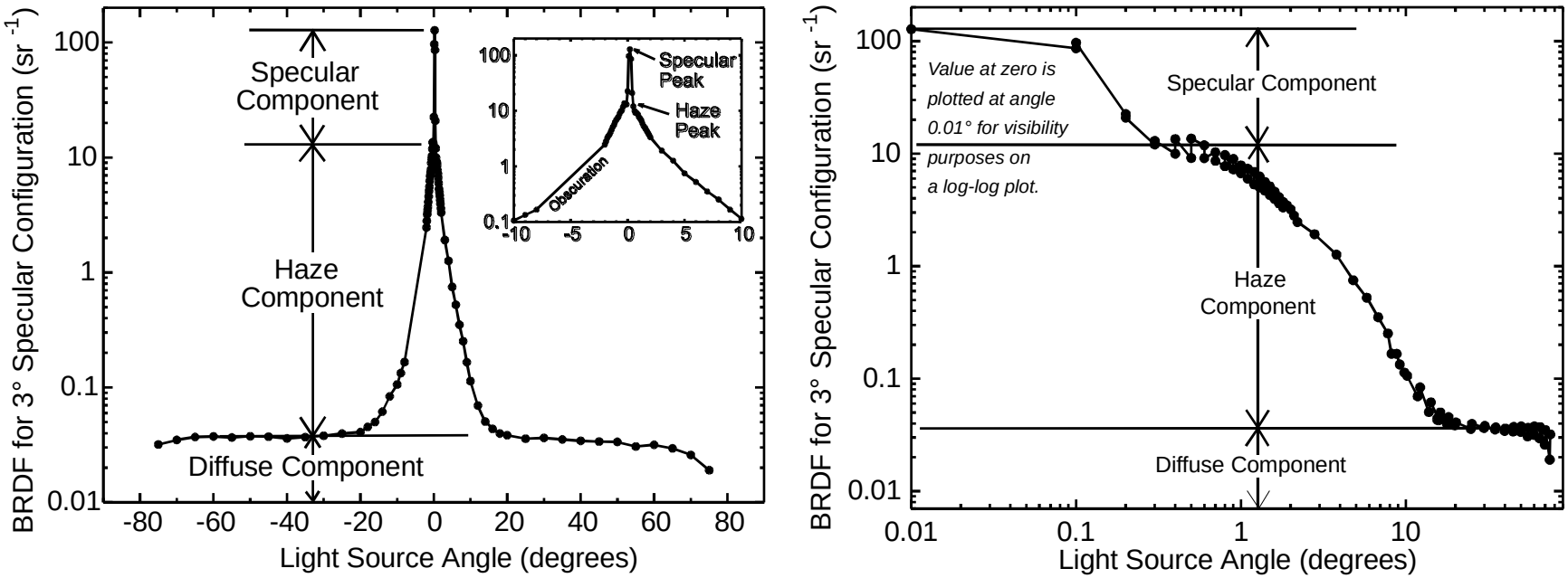

Fig. 2. *An in-plane BRDF of a sample material having all three components of reflection contributing non-trivially. The graph on the right is the same data using a log scale on the abscissa. We plot the q = 0° values at q = 0.01° so that they are visible on the graph. The negative q values are plotted as positive values. The data were collected with the detector at 3° using a point light source. The angle specifies the position of the light source as measured from the specular direction (at –3° from the normal) for which the angle is set to* $\theta = 0°$.

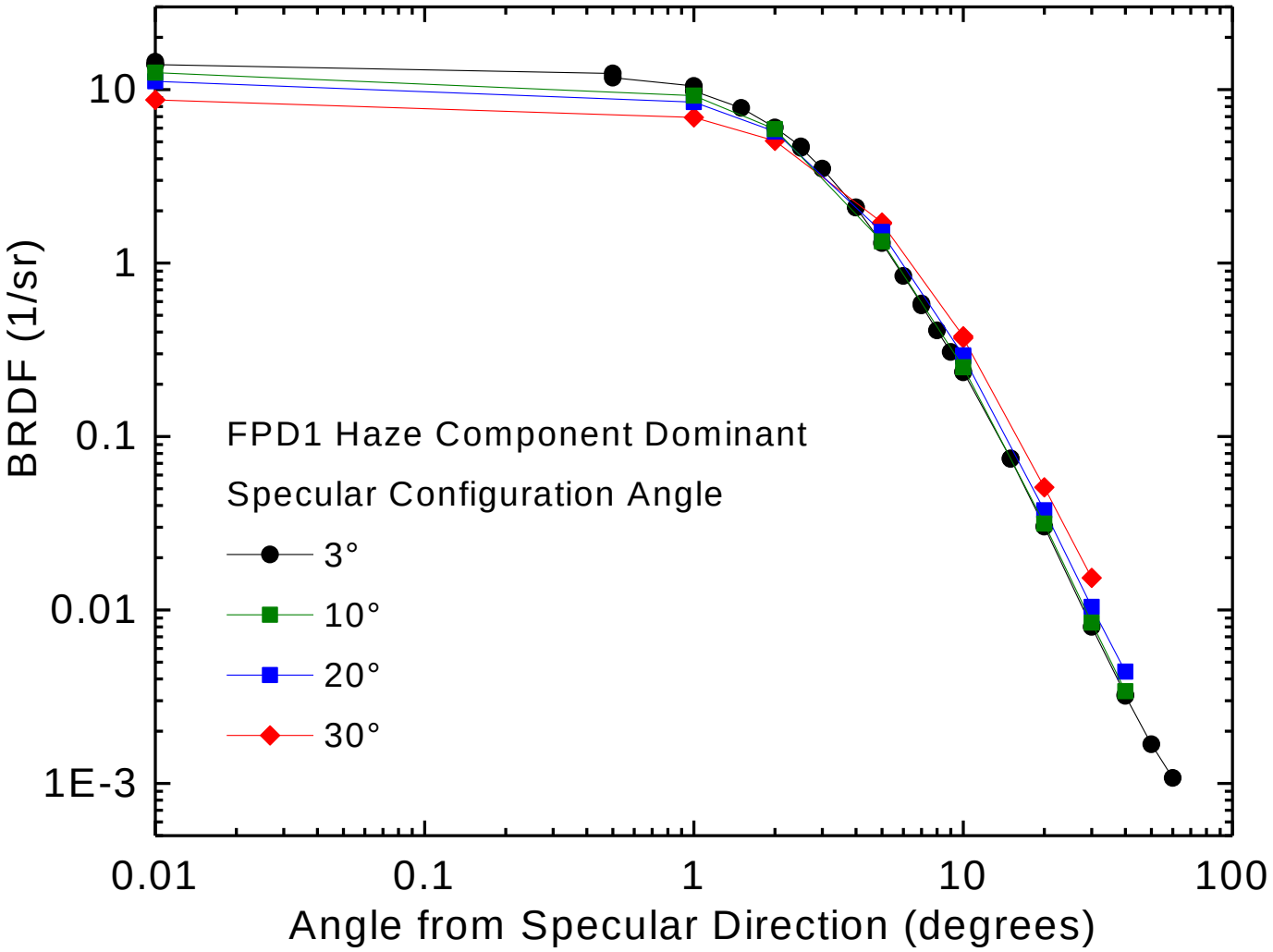

Fig. 3. *Comparison of BRDFs taken at different specular angles on the same display. Detector at 3°, 10°, 20°, and 30° from normal.*

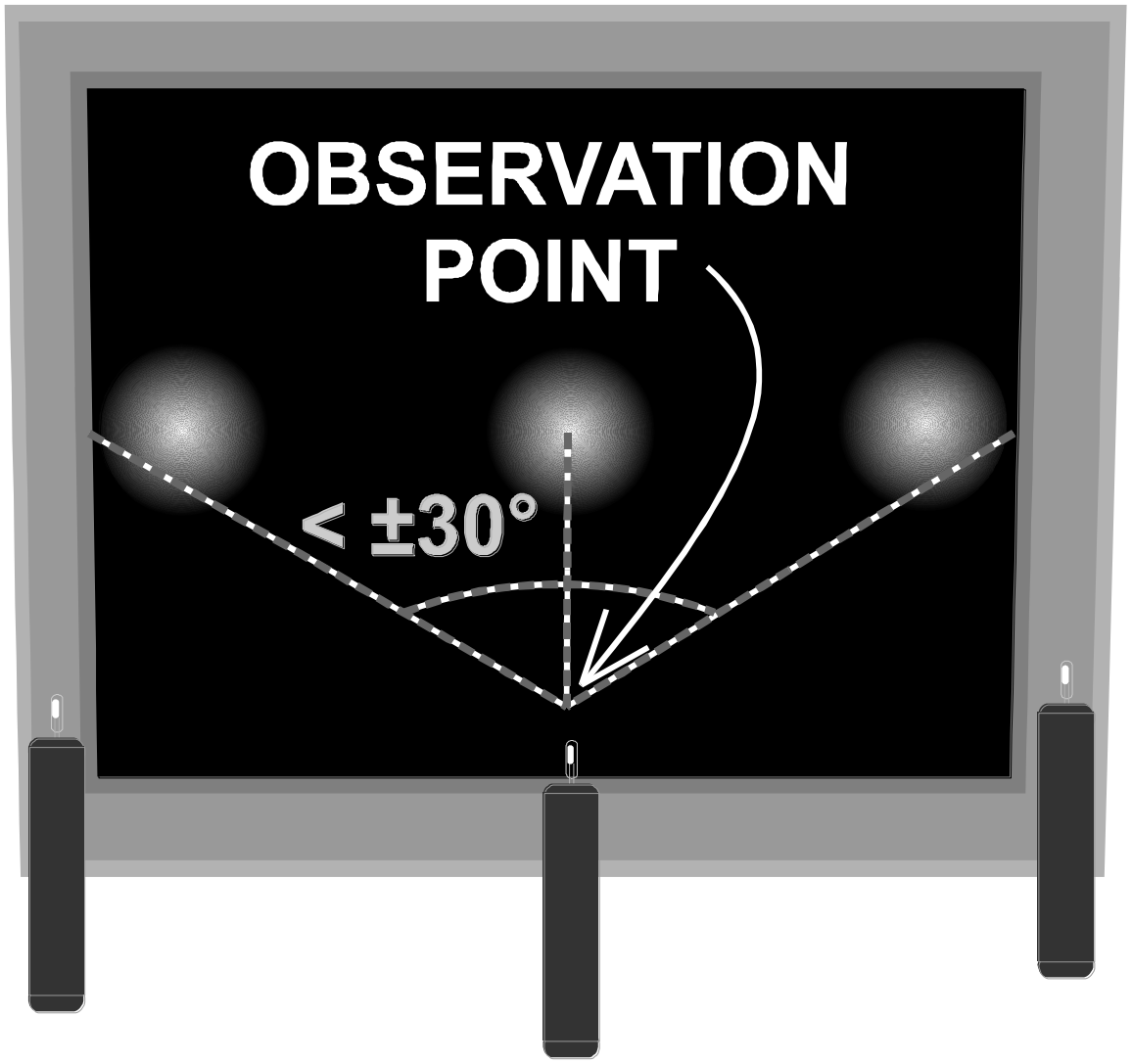

Fig. 4. *For many displays, the image of the source appears to have approximately the same shape as viewed at positions all over the screen from a single observation point near the normal.*

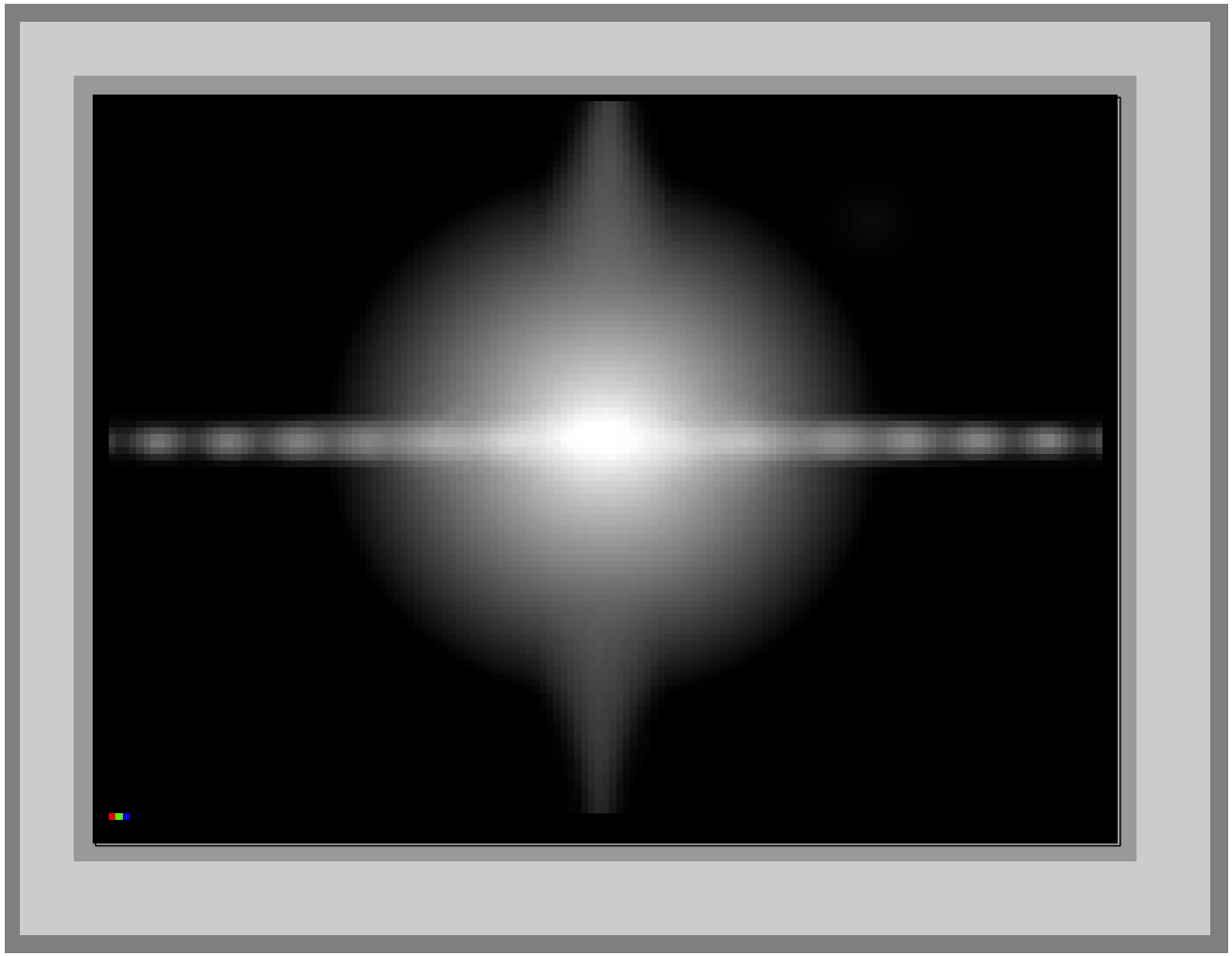

Fig. 5. *A display BRDF that is not symmetrical about the normal.*

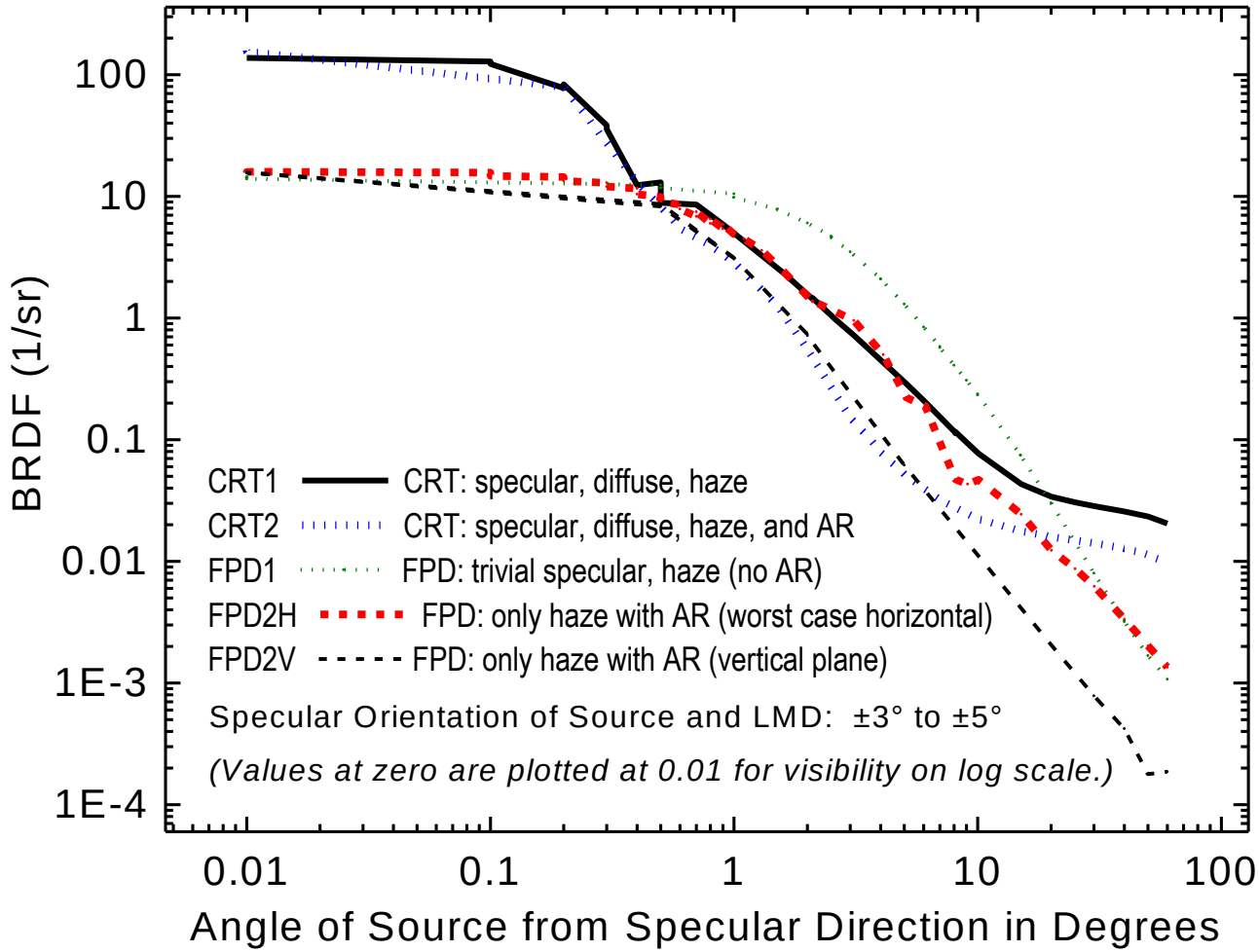

Fig. 6. *Comparisons of in-plane BRDFs for CRTs and FPDs. The data for the FPDs employed an apparatus with a 0.2° detector aperture. Both FPDs are LCDs.*

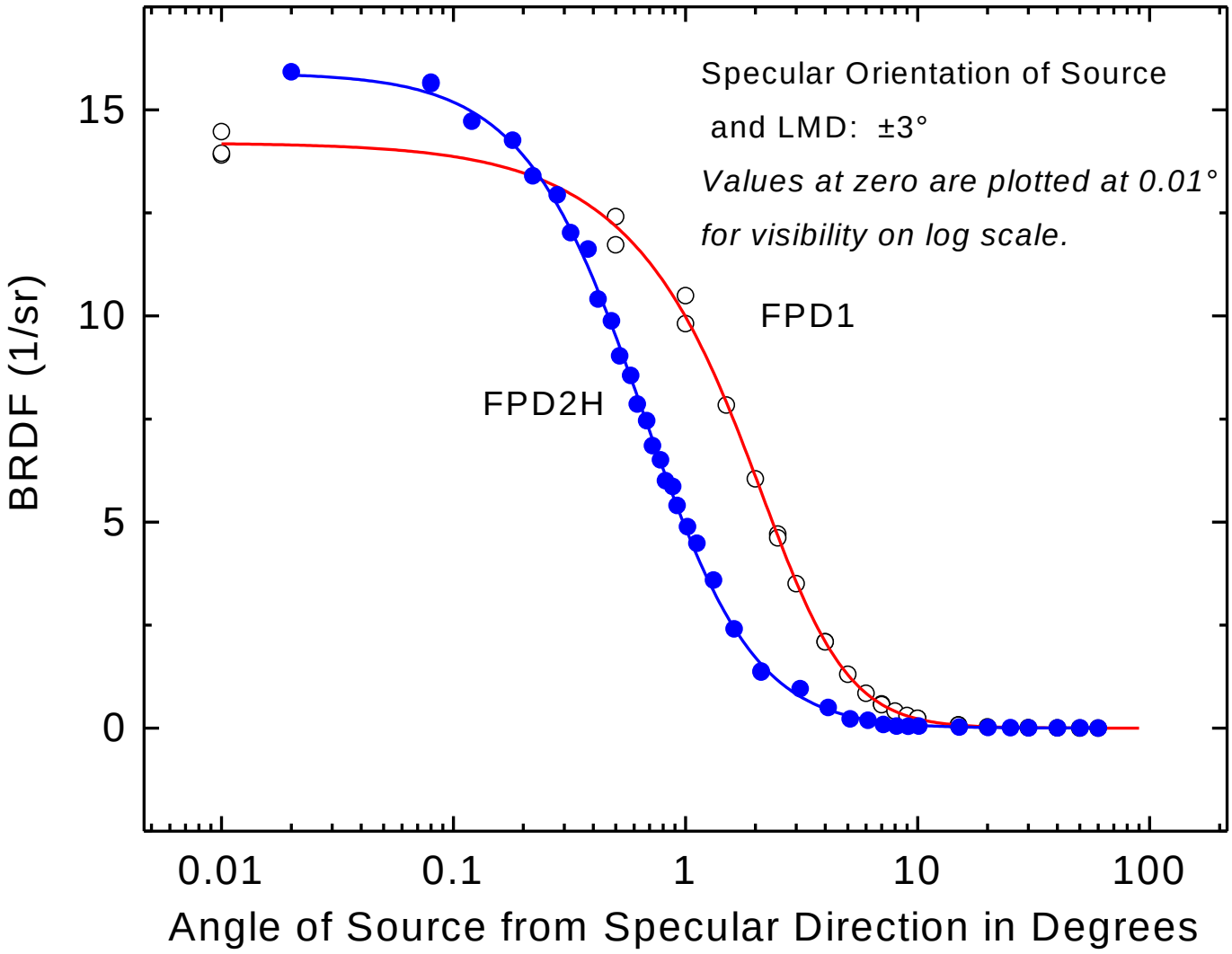

Fig. 7*. BRDF of FPD1 and FPD2H showing that the value of the BRDF can change substantially over even 0.5°.*

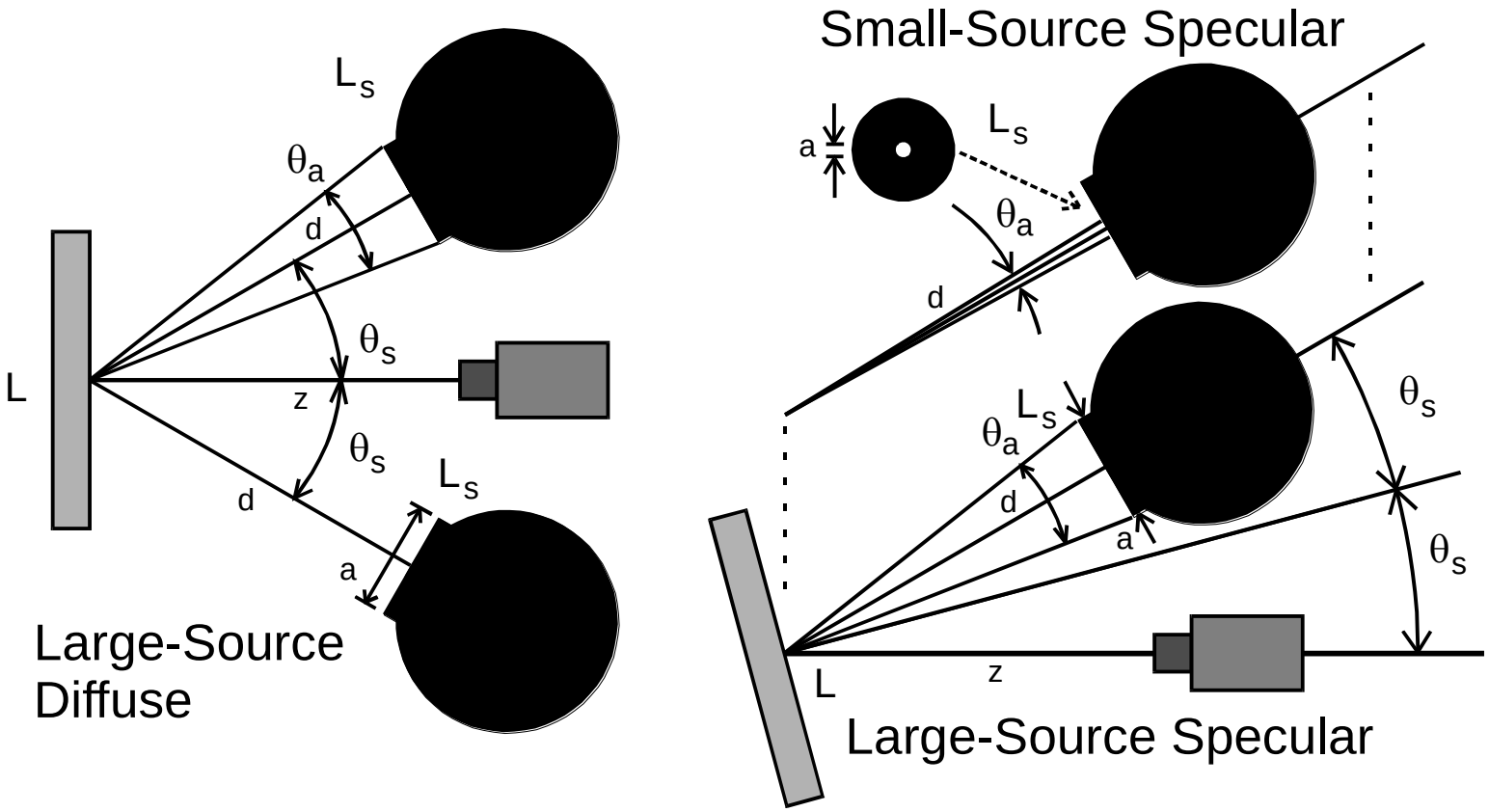

Fig. 8*. Common reflection measurement configurations.*

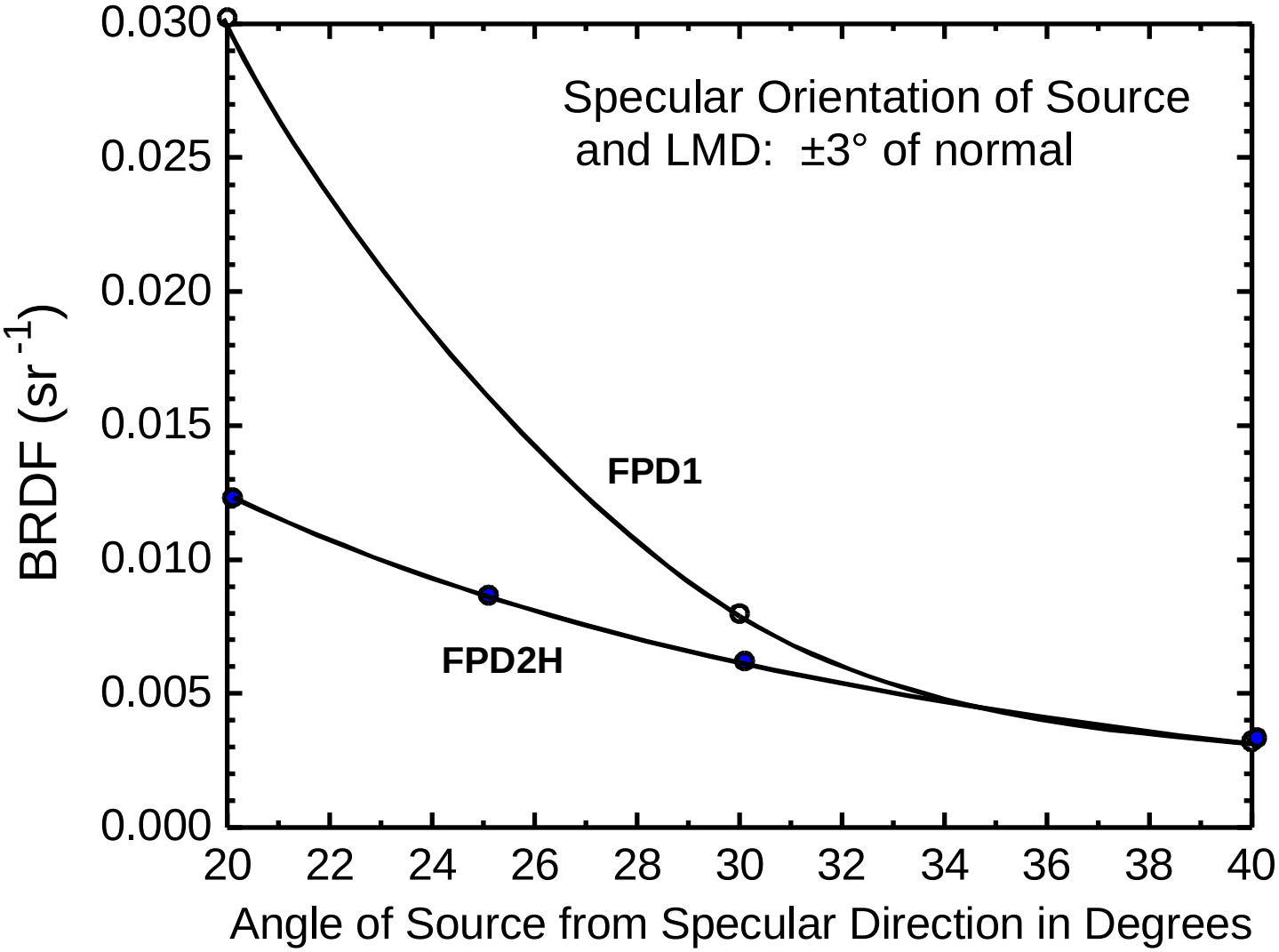

Fig. 9. *BRDFs off normal for two FPD surfaces.*

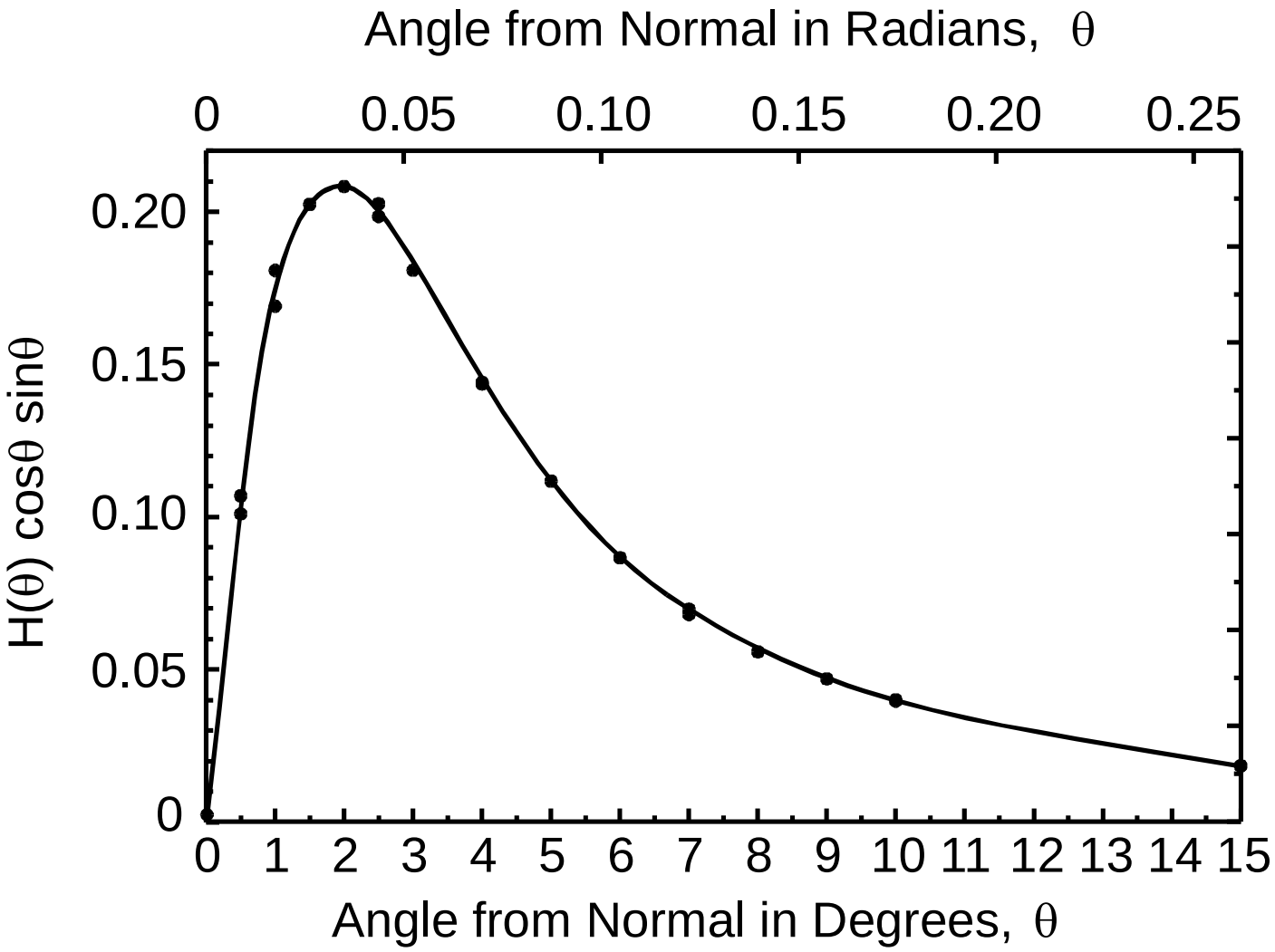

Fig. 10. *Integrand for large-source specular contribution from haze using the data for FPD1.*

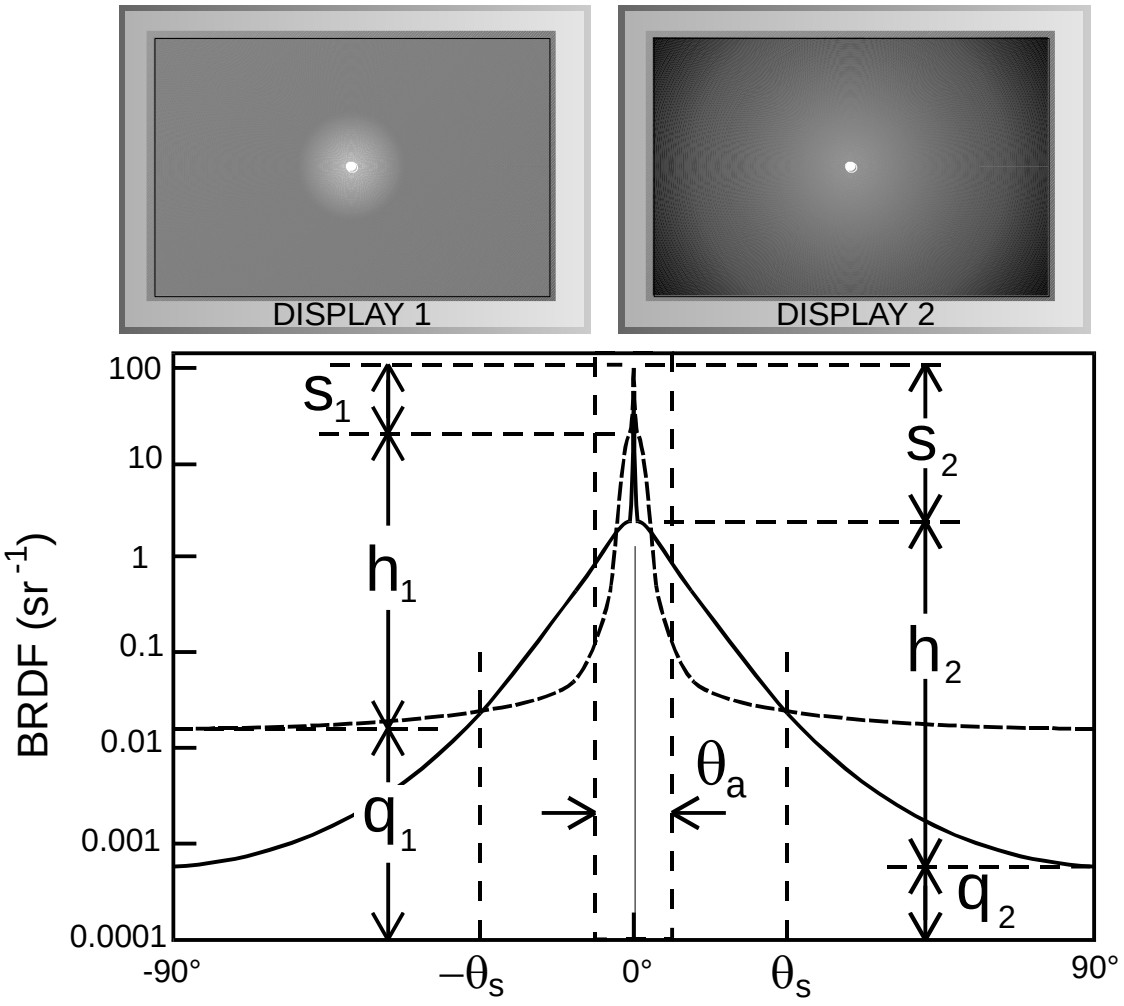

Fig. 11. *Two BRDFs that could produce the same measurement results using conventional techniques. However, the displays would appear very different to the eye if a point source were observed in the reflection as in the above images.*

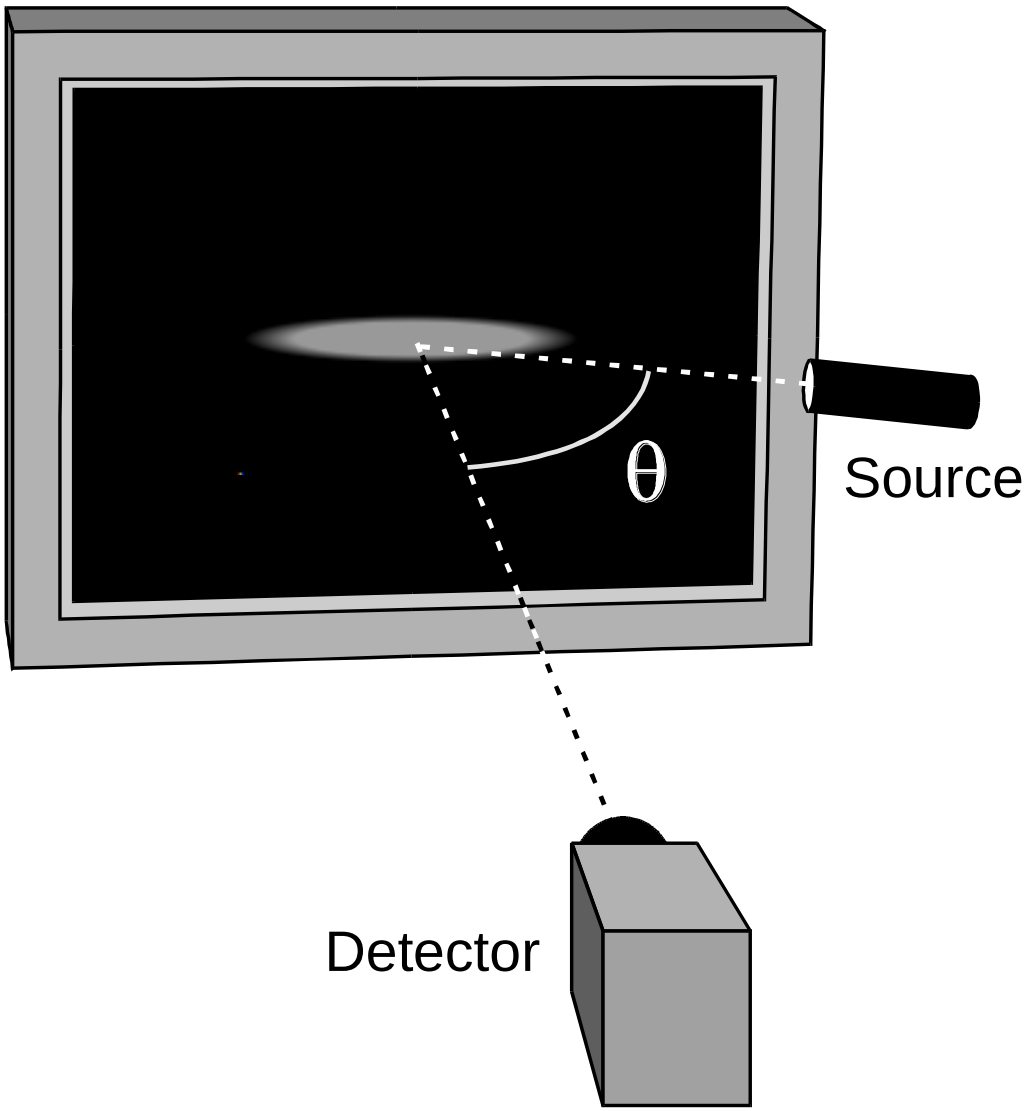

Fig. 12. *The diffuse (Lambertian) term, if non-trivial, will be indicated by the haze asymptotically reaching a constant as the angle of the light source from the normal increases toward 90°. Note that the detector would have to measure the entirety of the elongated illuminated area. Otherwise, the detector would have to measure within the illuminated area, correct the reading with* $1/\cos\theta$*, and the illumination would have to be very uniform over its cross-section.*

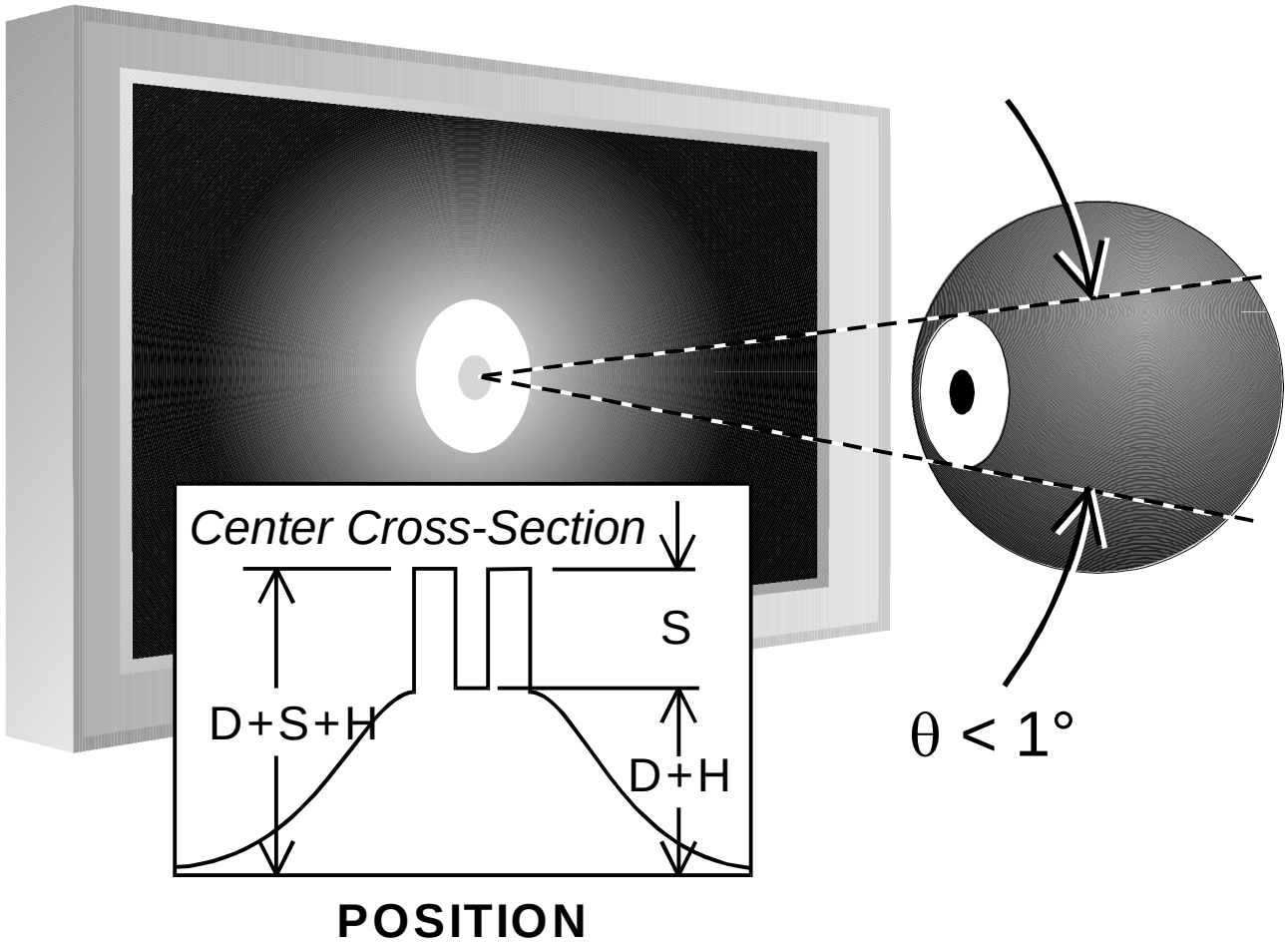

Fig. 13. *The haze peak added to the diffuse component may be observable at the center of an annulus that is sufficiently small. The specular component would be obtained with the same apparatus by subtracting off the haze peak and the diffuse component making appropriate corrections for glare.*

FIGURE CAPTIONS:

Fig. 1. Illustration of the three types of reflection found in modern electronic displays. B refers to the BRDF that can have a diffuse (Lambertian) component, D, a mirror-like specular component that produces a distinct image, S, and a haze component, H. At least one component must exist. There are four combinations of the three components. Any or all of the three components can exist nontrivially, or one component can dominate while the other two components make a trivial contribution to the reflection (as in the case of the first three illustrations).

Fig. 2. An in-plane BRDF of a sample material having all three components of reflection contributing non-trivially. The graph on the right is the same data using a log scale on the abscissa. We plot the q = 0° values at q = 0.01° so that they are visible on the graph. The negative q values are plotted as positive values. The data were collected with the detector at 3° using a point light source. The angle specifies the position of the light source as measured from the specular direction (at –3° from the normal) for which the angle is set to $\theta = 0°$.

Fig. 3. Comparison of BRDFs taken at different specular angles on the same display. Detector at 3°, 10°, 20°, and 30° from normal.

Fig. 4. For many displays, the image of the source appears to have approximately the same shape as viewed at positions all over the screen from a single observation point near the normal.

Fig. 5. A display BRDF that is not symmetrical about the normal.

Fig. 6. Comparisons of in-plane BRDFs for CRTs and FPDs. The data for the FPDs employed an apparatus with a 0.2° detector aperture. Both FPDs are LCDs.

Fig. 7. BRDF of FPD1 and FPD2H showing that the value of the BRDF can change substantially over even 0.5°.

Fig. 8. Common reflection measurement configurations.

Fig. 9. BRDFs off normal for two FPD surfaces.

Fig. 10. Integrand for large-source specular contribution from haze using the data for FPD1.

Fig. 11. Two BRDFs that could produce the same measurement results using conventional techniques. However, the displays would appear very different to the eye if a point source were observed in the reflection as in the above images.

Fig. 12. The diffuse (Lambertian) term, if non-trivial, will be indicated by the haze asymptotically reaching a constant as the angle of the light source from the normal increases toward 90°. Note that the detector would have to measure the entirety of the elongated illuminated area. Otherwise, the detector would have to measure within the illuminated area, correct the reading with $1/\cos\theta$, and the illumination would have to be very uniform over its cross-section.

Fig. 13. The haze peak added to the diffuse component may be observable at the center of an annulus that is sufficiently small. The specular component would be obtained with the same apparatus by subtracting off the haze peak and the diffuse component making appropriate corrections for glare.

REFERENCES:

[1] ASTM Standards on Color and Appearance Measurement, 5th edition, E 284-95a, "Standard Terminology of Appearance," definition of haze, p. 243, 1996.

[2] ASTM Standards on Color and Appearance Measurement, 5th edition, D 4449-90 (Reapproved 1995), "Standard Test Method for Visual Evaluation of Gloss Differences Between Surfaces of Similar Appearance," pp. 178-182, 1996. This discusses distinctness-of-image gloss and reflection haze.

[3] To be published.

[4] F. E. Nicodemus, J. C. Richmond, J. J. Hsia, I. W. Ginsberg, and T. Limperis, *Geometrical Considerations and Nomenclature for Reflectance*, NBS Monograph 160, National Bureau of Standards, Gaithersburg October 1977.

[5] M. E. Becker, "Evaluation and Characterization of Display Reflectance," Society for Information Display International Symposium, Boston Massachusetts, May 12-15, 1997, pp 827-830. Dr. Becker also makes reference here to the work by J. C. Stover, *Optical Scattering, Measurement and Analysis*, SPIE Optical Engineering Press, Bellingham, Wash., USA, 1995.

[6] E. F. Kelley and G. R. Jones, "Utilizing the Bidirectional Reflection [should be Reflectance] Distribution Function to Predict Reflections from FPDs," Society for Information Display International Symposium, Boston Massachusetts, May 12-15, 1997, pp 831-834.

[7] ASTM Standards on Color and Appearance Measurement, 5th edition, E 1392-90, "Standard Practice for Angle Resolved Optical Scatter Measurements on Specular or Diffuse Surfaces," pp. 439-444, 1996. This refers also to reference 8.

[8] ASTM Standards on Color and Appearance Measurement, 5th edition, E 167-91, "Standard Practice for Goniophotometry of Objects and Materials," pp. 206-209, 1996.

[9] Note that the data presented in this paper are for illustration purposes only. The combined standard uncertainty in all the present measurements is estimated to be ±10% of the measurand using a coverage factor of two.